Hardware Article

Open-source wideband (DC to MHz range) isolated current sensor

Burkhard Ulrich

Baden-Wuerttemberg Cooperative State University Stuttgart, DHBW Stuttgart Campus Horb, Florianstr. 15, 72160 Horb am Neckar, Germany

ARTICLE INFO

ABSTRACT

A low-cost open-source wideband current sensor, measuring currents in a frequency range from DC to 5 MHz, is proposed. The sensor provides galvanic isolation, low insertion impedance, and can be used together with an oscilloscope as replacement for an expensive current probe, or as circuit integrated sensor, to measure currents with peak values up to 20 A. The hardware of the sensor consists of standard parts soldered on a printed circuit board; no special custom parts and/or manufacturing steps are needed to build. Applications are general measurement and laboratory use, e.g. measuring current waveforms in lab experiments. But the sensor can also be integrated in control circuits requiring measurements of time varying currents, e.g. for high speed current mode control in power electronics.
© 2019 The Author. Published by Elsevier Ltd. This is an open access article under the CC BY license (http://creativecommons.org/licenses/by/4.0/).

Specifications table

Hardware name	*Open Source Current Sensor*
Subject area	• Educational Tools and Open Source Alternatives to Existing Infrastructure
Hardware type	• Measuring physical properties and in-lab sensors
Open Source License	*Creative Commons Attribution 4.0 (CC-BY)*
Cost of Hardware	25–35 €
Source File Repository	https://osf.io/d8u9a/

1. Hardware in context

1.1. Introduction

Current sensing is a basic task in a typical electronics or electrical engineering laboratory environment, but in contrast to voltage measurements, to observe current waveforms, more specialized equipment is needed. For example to measure time varying currents with an oscilloscope, a special current probe is required. These devices can be expensive; prices are ranging from several hundred up to several thousand euros, depending on the desired measurement bandwidth and current rating. E.g. in Table 1 an overview of some commercial available probes is given [20–22].

Table 1
Commercial current probes for oscilloscopes.

Type and manufacturer		Current range	Bandwidth	Sensitivity	Price
80i-110s	(Fluke)	0…±10 A or 0…±100 A	DC…100 kHz	10 mV/A or 100 mV/A	764 € [19]
I-Prober 520	(AIM-TTI)	±10 mA,.,± 10 A	DC…5 MHz	1 V/A	667 € [19]
N2893A	(Keysight)	0…± 15 A	DC…100 MHz	100 mV/A	3459 € [19]

Although commercial probes provide a convenient way for current measurement, these probes are often not an option for use in an undergraduate laboratory, when multiple workplaces have to be equipped, or if several probes are needed as part of an experimental setup. In this case a less expensive approach is to build your own current sensor. There are some open-source current sensors available [1,3,4,7,11], but these are either for relatively low frequencies (below 100 kHz) [1,3], or are based on shunt resistors providing no galvanic isolation [4,7]. For applications where pulsed currents at a voltage potential above ground have to be measured, e.g. research and education in power electronics and switch mode power supplies, there is a lack of useful open-source current probes. Although there are solutions presented [2,5,6,10] in research articles, these designs often require very special hardware, complicated assembly, and often not all the relevant information to build these sensors is provided. Another approach to build a current probe sensor is to use commercial current sensors, which are primarily intended for direct PCB integration. In Table 2 an overview of some of these sensors is given [23–25], for comparison the here proposed sensor is also listed.

1.2. Hardware and design objectives

As shown Table 2, current sensors for PCB integration are typically limited to frequencies below 1 MHz. Therefore an alternative approach is presented here, which combines a Hall effect sensor IC with a low cost PCB mounted current transformer to provide a:

- low-cost current probe alternative (factor 10–100 cheaper compared to commercial probes)
- easy to manufacture/assemble current sensor (double layer PCB with hand solderable components)
- sensor design employing only standard parts available from major distributors
- galvanic isolated sensor design
- current sensor with wide bandwidth from DC to several MHz (5 to 10 times larger compared to commercial PCB current sensors)
- measurement current range from mA to 10 A and higher

The use of standard components will heavily influence the sensor characteristics and restrict the performance once the parts are chosen. To alleviate this problem the proposed hardware is designed in a way, that the sensor characteristic can be easily adapted by interchanging some of the main components. E.g. by using another type of Hall effect sensor and/or current transformer the input current range, frequency response and sensitivity can be adapted to the user needs. To use the sensor in different applications (e.g. standalone sensor or as circuit integrated sensor), a simple design based on a single 5 V supply rail is proposed.

1.3. Sensor applications

Main applications for the current sensor are:

- low-cost replacement for oscilloscope current probes, especially for educational use
- use as circuit integrated current sensor for applications which require measurements of the actual current waveforms for control purposes, e.g. current mode control in power electronics
- versatile equipment for all sorts of lab current measurements

Table 2
Commercial PCB current sensors.

Type (Manufacturer)	Current Range	Bandwidth	Sensitivity	Price
ACS730 (Allegro)	0…±25 A up to 0…±65 A	DC…1 MHz	100 mV/A down to 30 mV/A	4,56 €* [18]
HLSR-P series (LEM)	0…±10 A up to 0…±100 A	DC…400 kHz	80 mV/A down to 16 mV/A	10,72 €* [18]
LA01P (TAMURA)	0…±35 A up to 0…±175 A	DC…400 kHz	60 mV/A down to 12 mV/A	11,69 €* [18]
Proposed Current Sensor	0…±10 A up to 0…±20 A	DC…5 MHz	100 mV/A up to 500 mV/A (adjustable)	25–35 €**

* Single quantity – device only.
** Price for PCB and device.

The sensor should be capable of measuring typically encountered waveforms in electronics and especially in power electronics. In these applications current waveforms need to be measured, which simultaneously contain DC, low frequency and high frequency (spectral) signal contents. E.g. the typical inductor current waveform of a DC/DC converter can be considered as the superposition of a DC component and a triangular waveform at a switching frequency f_s. Therefore a current sensor is needed, which is able to measure DC (or during dynamic transitions slowly varying AC components), and at the same time AC signal components at multiples of the switching frequency f_s. With today's switching frequencies in the range greater than 100 kHz a broadband current sensor, ranging from DC up to the MHz range, is needed to observe current waveforms in such a circuit.

2. Hardware description – overview and measurement principle

2.1. Overview and interfaces

Fig. 1 shows the PCB of the proposed current sensor, identifying the main components and interfaces. Fig. 2 further indicates a simple system block diagram of the sensor. There are three connections to interface the sensor with the environment. First, the current I_M to be measured has to flow through pin headers J1 and J2 on the left side. Current I_M flows through the series connection of a pulse current transformer and a Hall effect current sensor, which converts the current I_M in an output voltage $V_{S,out}$. These are added up to achieve a wide bandwidth frequency response, as explained in the following section. The converted sensor output voltage signal $V_{S,out}$ is guided to a coaxial output connector J6 for interfacing to an oscilloscope. The third connection at pin header J3 in the upper right is the input terminal for an isolated power supply, typical a battery (e.g. 9 V), to power the signal processing circuitry.

Viewing the sensor as a system, the input output relation can be specified as

$$V_{S,out} = K_S \cdot I_M + V_{offset} \tag{1}$$

Here K_S denotes the sensor gain and V_{offset} the output voltage level with zero input signal. With the design values used in the following sections, K_S will be 0.1 V/A and V_{offset} either 0 V or 2.5 V.

The signal levels and main sensor characteristics are summarized in the following Table 3. Fig. 3 shows the ideal transfer characteristics of the sensor when evaluating Eq. (1) for the given values.

2.2. Measurement principle of proposed current sensor

Fig. 4 depicts a block diagram to explain the basic measurement principle of the proposed current sensor. It is built around two different current sensors, a commercial isolated Hall effect current sensor for the DC to low frequency signal content and a standard current transformer for the high frequency content. The measurement principle is similar to that described by Dalessandro et al. in [5], where a custom build current transformer containing an air gap with a Hall sensor
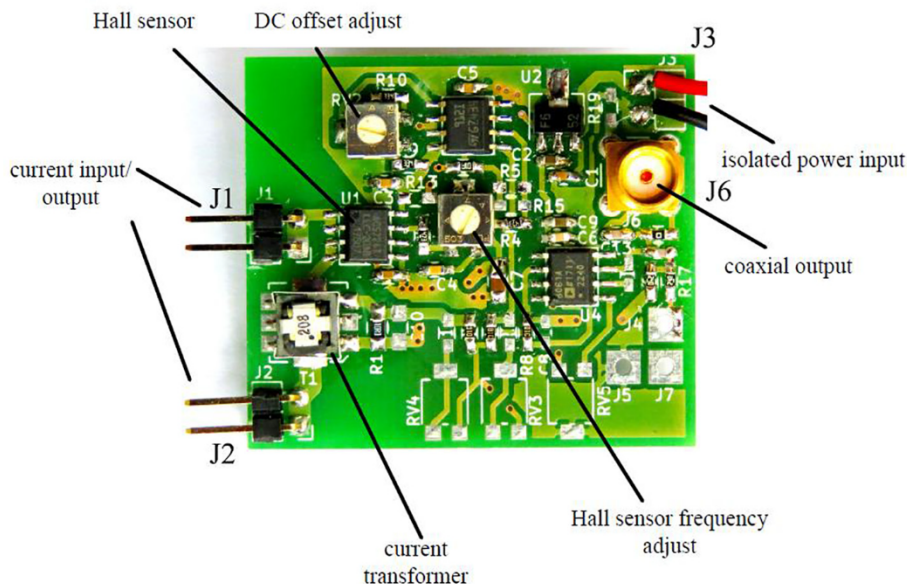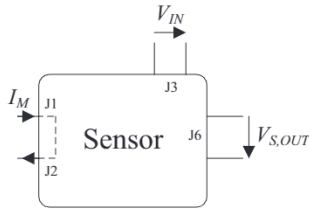

Fig. 1. Current sensor PCB.

Fig. 2. Basic block diagram illustrating the interfaces of the current sensor.

Table 3
Sensor characteristics and voltage/current levels at PCB terminals.

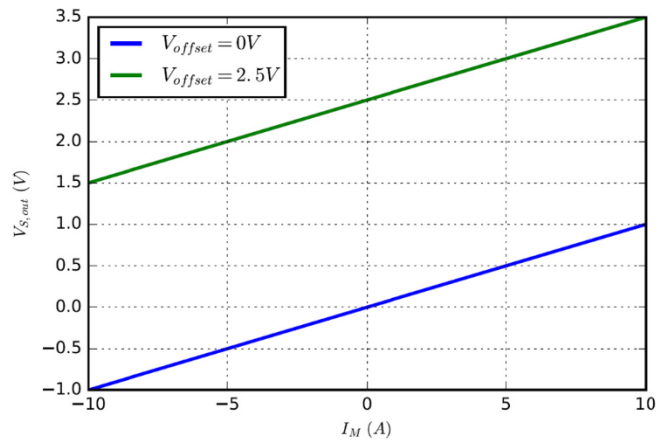|	
J1-J2 input current range I_M	typ. -10 A to $+10$ A (adjustable ±2.5 A to ±20 A)
J6 output voltage range $V_{S,out}$	-2.5 V...$+2.5$ V (0...5 V)
J3 power supply input voltage V_{IN}	7...20 V (DC)/supply current typ. 23 mA
Sensor sensitivity	typ. 0.1 V/A (adjustable 0.1 V/A to 1 V/A)
Sensor bandwidth	typ. 0 Hz...5 MHz (-3 dB)

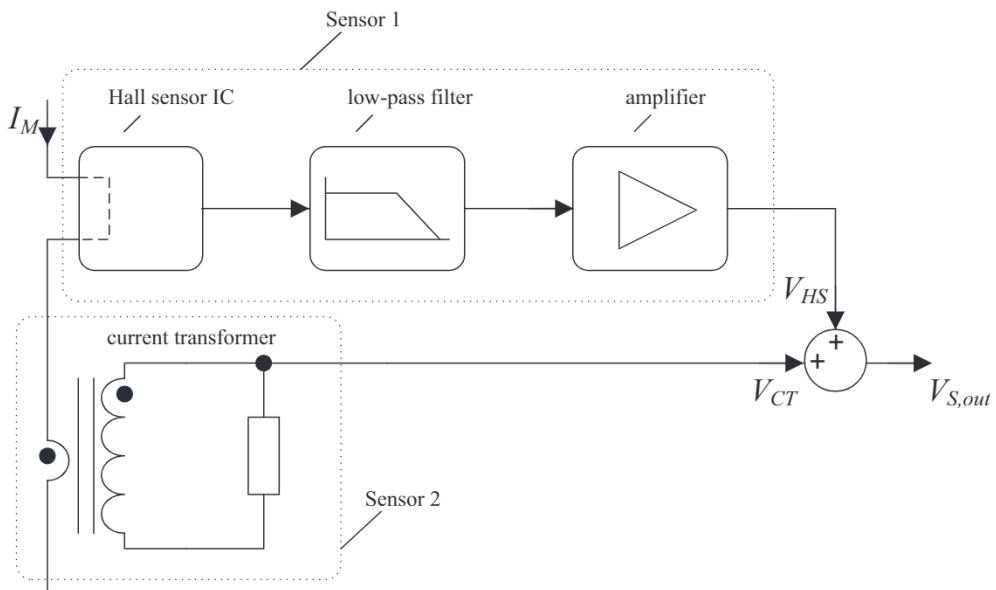**Fig. 3.** Ideal current sensor transfer characteristics.

Fig. 4. Block diagram illustrating the basic operating principle of the current sensor.

is used. Other approaches are presented by Velsink [8], also combining a Hall sensor and a current transformer on a single core with an airgap, and by Karrer, Hofer-Noser [6], where a Rogowski coil is combined with a Hall effect sensor to build a wideband sensor. These designs all rely on custom manufactured sensor components. In contrast here two independent commercial available sensor components are used.

As shown in Fig. 4, the current I_M which has to be measured is detected by both sensors. The frequency response of the Hall sensor is artificially reduced by an external low-pass filter. This forces a sensor output voltage V_{HS} of the Hall effect current sensor which has a cutoff frequency solely determined by the external filter. The following amplifier ensures that no change of the cutoff frequency due varying signal amplitudes or loading occurs. A second sensor voltage signal V_{CT} from a current transformer is added to the filtered Hall sensor voltage V_{HS} to generate the sensor output signal $V_{S,out} = V_{HS} + V_{CT}$. If the corner frequency of the low-pass filter is set properly, than the overall system response

$$G(f) = \frac{V_{S,out}}{I_M} = G_{CT}(f) + G_{HS}(f)$$

(2)

of the sensor will be flat to a high upper frequency, determined by the current transformer. In Eq. (2) $G_{CT}(f)$ is the transfer function of the current transformer and $G_{HS}(f)$ the combined transfer function of the Hall effect sensor and the following low-pass filter.

Assuming the external low-pass dominates the transfer characteristic, then $G_{HS}(f)$ can be approximated as a first order low-pass filter transfer function

$$G_{HS}(f) = \frac{V_{HS}}{I_M} = K_{HS} \frac{1}{1 + j \cdot \frac{f}{f_{HS}}}$$

(3)

with gain K_{HS} and corner frequency f_{HS}.

To calculate $G_{CT}(f)$, a simplified circuit model for a current transformer, neglecting losses, leakage and capacitive effects, is shown in Fig. 5.

From this circuit the transfer function $G_{CT}(f)$ can be approximated as a first order high-pass filter:

$$G_{CT}(f) = \frac{V_{CT}}{I_M} = K_{CT} \frac{j \cdot \frac{f}{f_{CT}}}{1 + j \cdot \frac{f}{f_{CT}}}$$

(4)

with gain $K_{CT} = \frac{N_S}{N_P} R_B$, lower corner frequency $f_{CT} = \frac{1}{2\pi} \frac{R_B}{L_S}$, secondary inductance L_S, burden resistance R_B and secondary/primary turns ratio N_S/N_P.

If Eq. (2) is evaluated using (3) and (4) with $f_{CT} = f_{HS}$ and $K = K_{CT} = K_{HS}$, the overall transfer function becomes a constant gain block with $G(f) = K$. The relationships (2), (3) and (4) are shown in Fig. 6 for a value of $K = 1$.

Ideally, a flat frequency response from DC up to high frequencies can be achieved. In practice, the frequency response of the current transformer is influenced by parasitic elements. Therefore, the usable bandwidth is limited at high frequencies.

As already mentioned, the principle for adding two sensor signals is commonly used to realize current sensors with a wide bandwidth ranging from DC to the MHz range [5,6,8,10,28,29]. In contrast to the existing solutions, here standard components are used to build the current sensor. The key concept for a simple sensor design is to use a standard isolated Hall effect sensor IC for measuring the low frequency part and combining it with a commercial off-the-shelf high bandwidth current transformer for the high frequency signal content. Therefore the property of having a non-invasive current sensor is lost, but a very low-cost sensor can be built, with standard parts on a PCB. The resultant sensor behaves like the known open-source isolated Hall effect current sensor boards [3,11], but with a drastically increased bandwidth.
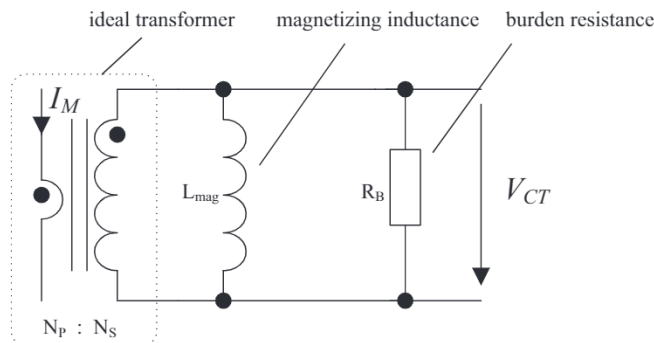

Fig. 5. Simplified current transformer equivalent circuit for modelling frequency response.
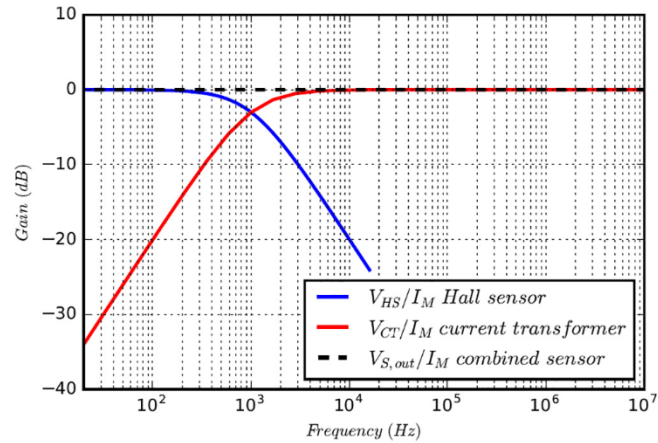
Fig. 6. Transfer functions according to Eqs. (2)–(4).

3. Detailed hardware description

The full schematic of the current sensor is shown in Fig. 7. It consists of three parts:

- power input and a linear voltage regulator for generating an internal V_{CC} = 5 V power supply
- a rail splitter circuit generating a virtual ground signal at V_{REF} = 0.5V_{CC}
- the signal processing and sensor circuit

Not all components shown in the schematic are needed, some are marked as DNP (do not populate) in the schematic. An overview of these components is given in Table 4.These ancillary components are used for modifications, as will be described in the following paragraphs, which discusses the schematic in detail.

3.1. Power input and linear voltage regulator

The power supply of the sensor is shown in Fig. 8. It uses a standard linear voltage regulator (type 78L05), which generates a constant 5 V supply rail from an isolated input voltage between 7 V and 20 V. The input voltage should be applied between connection J3.1 und J3.2. Isolation of the supply is required, as the sensor output signal is either referenced to the power supply ground (GND) or to a reference voltage (VREF = GND + 2.5 V). A battery is recommended for operation as a standalone current sensor, e.g. a standard 9 V battery can be used. For applications where the sensor is integrated in a circuit, the voltage regulator can be replaced by a short between pin 3 and pin 1 of U2, and then a single 5 V power supply is sufficient to power the sensor. Therefore it can be easily integrated in control circuits powered by a single 5 V rail.
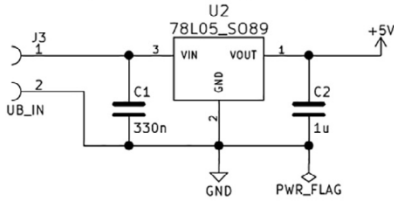
3.2. Op amp rail-splitter

The second block of the sensor circuit, shown in Fig. 9, is an op amp based rail-splitter circuit. U3B is configured as a unity gain buffer amp, which amplifies the output of the voltage divider circuit composed of R9, RV2 and R10. R11 isolates the op amp output from capacitor C7, to avoid instability due to capacitive loading. Voltage VREF at C7 should be about half the supply voltage (approx. +2.5 V) and can be adjusted by trimmer RV2. VREF is used as a sort of virtual ground as reference voltage for the sensing circuit. For bidirectional output voltages, the sensor's output signal may be referenced to VREF. For unidirectional output, VREF sets the output level for a zero input current.

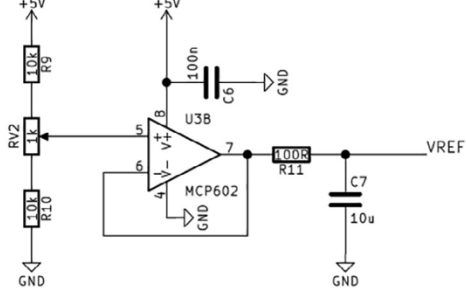### 3.3. Sensor circuit and signal processing

The signal processing circuitry, which is shown in the lower part of Fig. 7, constitutes the largest part of the sensor. It can be further divided into four sections:

- Hall effect current sensor and its signal processing interface (Fig. 10)
- current transformer interface (Fig. 11)
- inverting summing amplifier for signal mixing (Fig. 12)
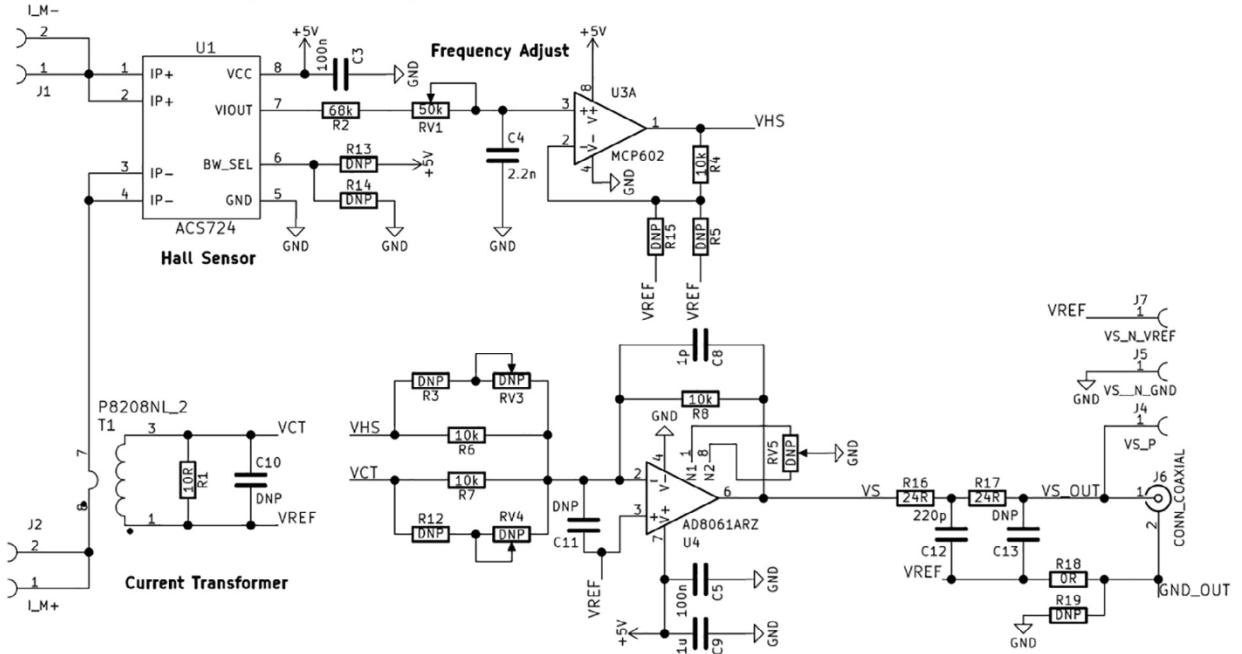- output connection (Fig. 13)

Fig. 7. Full schematic of the proposed current sensor – upper left: linear voltage regulator – upper right: DC rail splitter circuit – lower part: signal processing and sensor circuit.

Table 4
Ancillary components.

Component Ref Designators	Influenced circuit property
R13, R14	Bandwidth selection Hall effect sensor
R5, R15	Adjusting gain of Hall effect sensor signal path
C10	High frequency compensation/limitation current transformer
R3, RV3	Optional resistor and trimmer for gain adjustment of Hall sensor output at summing amplifier
R12, RV4	Optional resistor and trimmer for gain adjustment of current transformer output at summing amplifier
C11	Capacitor for adjusting frequency response of summing amplifier
RV5	Trimmer for offset compensation of summing amplifier op amp (if provided by manufacturer)
C13	Capacitor for high frequency low-pass at sensor output
R18, R19	Output reference level selection (0 V or VREF)

Sensed current I_M flows either into J1 and out of J2 or vice versa, passing through both sensors, the Hall sensor U1 and the current transformer T1, which are both shown on the left side of Fig. 7. U1 is a galvanic isolated Hall effect current sensor with a ratiometric output voltage. Suitable versions are for example ACS723 or ACS724 current sensors in versions with ±20 A bidirectional current range. The output of these sensors will be at half the supply voltage at zero input current. If the model ACS723 is used, either R13 or R14 could be mounted, setting the bandwidth of the Hall effect sensor. If ACS724 is used, R14 can be replaced by a capacitor for filtering and R13 should be omitted. But it is not recommended to populate R13 and R14,
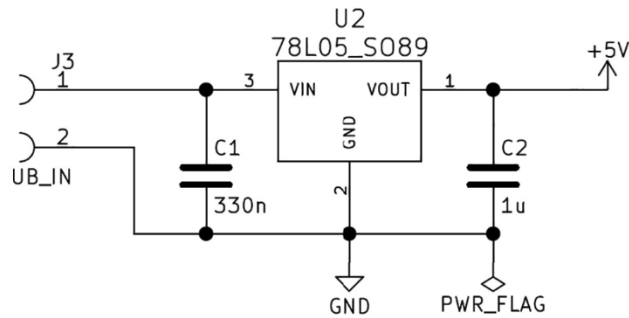
Power Input and Voltage Regulator

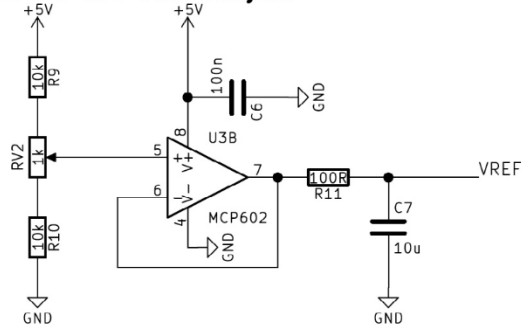**Fig. 8.** Power input circuit.

Rail Splitter DC and Offset Adjust

Fig. 9. Op amp rail-splitter circuit.
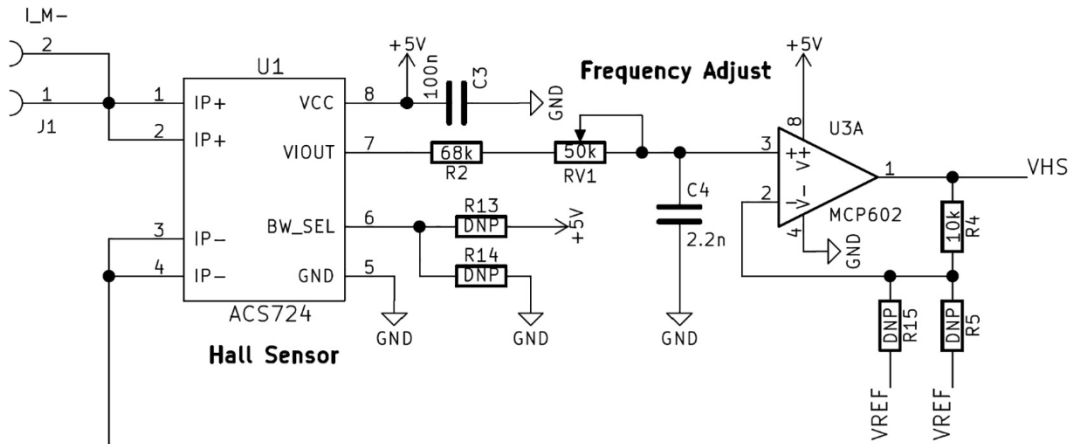
Fig. 10. Hall effect current sensor and interface circuit.

because this influences the frequency responses in a way which cannot be compensated easily. R2, RV1 and C4 form the first order low-pass filter, to actually let the user set the upper cutoff frequency f_{HS} of the Hall sensor in the range:

$$613\,\text{Hz} = \frac{1}{2\pi \cdot (R_2 + R_{V1}) \cdot C_4} < f_{HS} < \frac{1}{2\pi \cdot R_2 \cdot C_4} = 1064\,\text{Hz}$$

Here RV1 is the adjustable value of the trimmer pot. Op amp U3A performs two tasks; first, it decouples any load from the low-pass filter, and second, it allows setting an additional gain in path of the Hall effect current sensor, if optional resistors R15 and/or R5 are populated. In the actual design, this is not needed if the used Hall sensor has a sensor gain of $K_{HS} = 0.1$ V/A, which is case for the use of the recommended Hall effect current sensors.

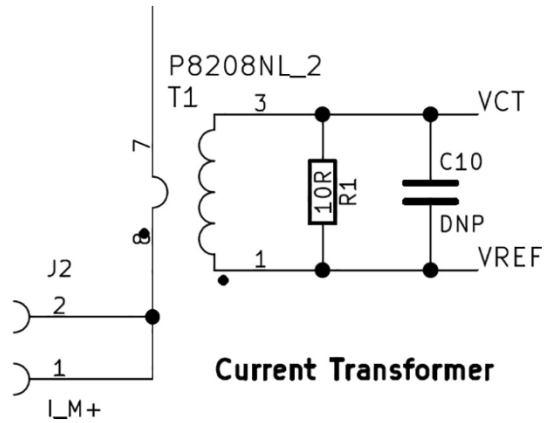**Fig. 11.** Current transformer and interface circuit.
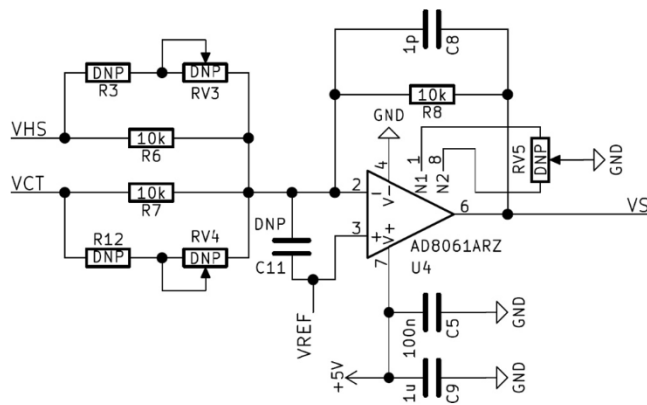

Fig. 12. Inverting summing amplifier for sensor signal mixing.
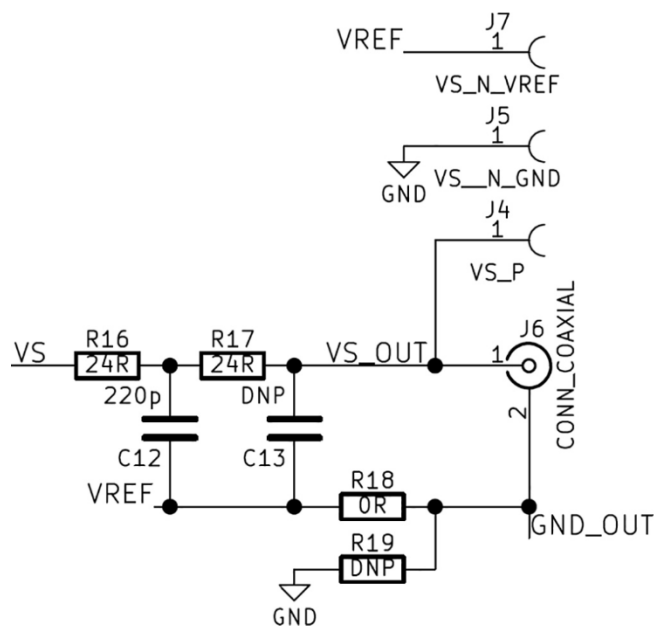

Fig. 13. Output connection.

In Fig. 11 the current transformer circuit is shown. T1 is a P820xNL series type current sense transformer from Pulse Electronics. The actual type P8208NL shown in the schematic has a turns ratio of $N_S = N_P = 100:1$, and a maximum rated current of 10 A. R1 is a 10 Ω burden resistance (R_B) of the current transformer, defining here an ideal sensor gain of

$$K_{CT} = 0,1 \frac{V}{A} = \frac{N_P}{N_S} \cdot R_B$$

for the current transformer. C10 can be used to short high frequency signals for noise suppression, but this will also reduce the bandwidth of the sensor. The output of the current transformer is the voltage across R1. As pin 1 of the current transformer is tied to VREF, the output voltage is shifted about +2.5 V (or half the supply voltage of the circuit). The ideal lower corner frequency can be calculated with the secondary inductance value of $L_S = 2$ mH from datasheet to

$$f_{CT} = \frac{1}{2\pi} \frac{R_B}{L_S} = 796 \, Hz$$

This value is in the range, which can be adjusted by the low-pass filter after the Hall sensor. Therefore frequency compensation can be accomplished. If another combination of current transformer and burden resistance is used, the values of R2, RV1 and C4 have to be adjusted properly.

The op amp circuit around U4, shown in Fig. 12, is an inverting summing amplifier, which adds up both sensor outputs, VHS and VCT, and also amplifies the sum of these signals. If resistors R6 and R7 are used, they define a constant gain of -R8/R6 for the Hall sensor output signal VHS and a gain of -R8/R7 for the current transformer output VCS. If adjustment is needed, the parallel connected paths, consisting of R3 and RV3 or R12 and RV4, should be used. R6, R7, and R8 should be precision resistors with a tolerance of 0.1% or less, as the resistance mismatch directly influences the sensor gain. In contrast to the other used op amps, U4 needs to be an amplifier with a large gain bandwidth product, especially if a large signal gain at high frequencies is needed. There are some optional components: capacitor C11 can be used to improve the frequency response of U4, this is needed if e.g. an AD817 is used for U4. Trimmer RV5 can be used to compensate the input offset voltage of U4, if these connections are provided by the IC. Capacitor C8 allows setting a cutoff frequency for a low-pass filter, formed by U4 and the gain setting resistors.

Fig. 13 shows the output stage of the sensor circuit. VS represents the summed sensor signal, which is fed into the cascaded second order low-pass filter, formed of R16, R17, C12 and C13. This filter performs two tasks; first it can be useful, if high frequency noise in the sensor signal VS needs to be suppressed; second R16 and R17 are used as a source termination resistance of a transmission line, connected at the coaxial connector J6. Therefore, the sum R16 + R17 of the resistor values should be approximately equal to the characteristic impedance of the cable connected to the output connector J6. Two 24 Ω resistors are used, as a coaxial cable with 50 Ω characteristic impedance was utilized.

Optional 0 Ω resistors R18 and R19 allow connecting either GND (0 V) or VREF (+2.5 V) to the common terminal GND_OUT of the SMA type coaxial output connector. E.g. when using the sensor as an oscilloscope current probe, R18 should be populated as then a bipolar output signal between −2.5 V to 2.5 V is available at J6. If the sensor is used as a circuit integrated sensor, R19 could be used instead of R18, as then a unipolar output signal between 0 and 5 V is available. As an alternative to the coaxial connector, three solder pads J4, J5, and J7 are available for direct soldering of cables.

3.4. Selection criteria for main components and customization

The sensor characteristics heavily depend on four main components, current transformer T1, Hall effect sensor U1, and op amps U3 and U4. In Table 5 the main selection criteria, sensor characteristics which are influenced, and some suitable parts for these components are listed.

To customize the sensor characteristics, e.g. for changing sensor sensitivity or current rating, essentially the Hall effect sensor U1 and the current transformer T1 or its burden resistance R1 have to be changed. Both components (U1 and T1) are available in several variants, e.g. with different sensitivity or turns ratio, but with identical footprint. Therefore, there are many possible variants, but the following should be considered:

- Sensitivity should not be changed by simply adjusting the gain of the summing amplifier. This can lead to a reduced sensor bandwidth and also to increased low frequency noise, because the Hall sensor output noise is amplified. Therefore, a suitable Hall sensor with sensitivity close to that required should be selected. Also both amplifiers (U3A and U4) in the signal chain should have a gain near unity.
- If the secondary-side inductance or the load resistance of the current transformer is changed, then its lower cutoff frequency is altered. In this case, the low-pass filter at the output of the Hall effect sensor must be adjusted accordingly.
- The required corner frequency of the low-pass following the Hall sensor should be at least one decade lower as the cutoff frequency of the Hall sensor. This is necessary to achieve a frequency response dominated by a first order low-pass characteristic.
- The upper frequency limit of the proposed sensor is limited by the parasitic characteristics of the current transformer. Therefore, the use of other types of current transformers may require additional investigations to assure the upper frequency limit of the current sensor.

In Table 6 some tested example customizations together with the resultant changes in sensor characteristics are listed.

Table 5
Main components and selection criteria.

Component	Selection criteria and sensor characteristics which are influenced

T1	• Primary current rating limits sensor input current range.
	• Upper cutoff frequency is determined by transformer parasitic properties. The high frequency behavior is often not directly specified by manufacturers, therefore a type with usable frequency range up to 1 MHz is chosen. The listed parts have a cutoff frequency much larger than 1 MHz.
	• A low value burden resistance increases the bandwidth.
	• The nominal secondary inductance defines the lower cutoff frequency; therefore this has to be chosen, together with burden resistance to be much lower than the bandwidth of the Hall effect current sensor.
	Tested parts: P820xNL Series (Pulse Electronics)
	                  PA1005.XXXNL Series (Pulse Electronics)
	                  5300 Series (Murata)

U1	• Current rating limits sensor input current range.
	• Bandwidth should be much larger as lower cutoff frequency of current transformer.
	• Low frequency behavior regarding linearity, accuracy and noise is determined by Hall effect sensor.
	• A 5 V type for simple system design is chosen.
	Tested parts: ACS724 Series (Allegro)
	                  ACS723 Series (Allegro)
	                  Caution: Bidirectional types are needed.

U3	• Rail-to-rail input and output needed. • Bandwidth 1 MHz or better. Tested parts: MCP602 (Microchip) TS921 (ST Microelectronics)

U4	• Rail-to-rail input and output needed.
	• High-speed-type required with bandwidth greater than upper cutoff frequency of transformer, otherwise this op amp will limit the upper frequency of the sensor. In particular, if additional gain is required, the bandwidth has to be increased further. Therefore, types with GBW > 50 MHz are considered.
	• Op amp should be unity gain stable.
	Tested parts: AD817 (Analog Devices)
	                  AD8061 (Analog Devices)
	                  OPA356 (Texas Instruments)

3.5. Components influencing sensor accuracy

The sensor accuracy is mainly influenced by

- the Hall sensor accuracy, e.g. for Hall sensor IC ACS724LLC-20AB a total output error of ±2% is specified for a temperature range of 25 °C...150 °C [30]
- burden resistance R1 of the current transformer
- gain setting resistors R4, R5, and R15 of noninverting amplifier U3A
- gain setting resistors R6, R7, and R8 of inverting summing amplifier U4
- input offset voltages and bias currents of op amps U3A and U4 will lead to a DC voltage offset error, which can be compensated by RV2, when the output signal is referenced to VREF
- if the sensor is used with an oscilloscope, the main limiting factor can be the scopes input circuitry, which can limit resolution and accuracy especially at low signal levels

Table 6
Example customizations.

No.	Major components		Sensor characteristics	
1	T1: P8208NL U1: ACS724LLC-20AB-T R1: 10R	(Pulse Electronics) (Allegro Microsystems) (various)	current range sensitivity output voltage	−10 A...10 A (limited by T1) 0.1 V/A 1.5 V...3.5 V (−1 V...1 V)
2	T1: PA1005.100NL U1: ACS724LLC-20AB-T R1: 10R	(Pulse Electronics) (Allegro Microsystems) (various)	current range sensitivity output voltage	−20 A...20 A (limited by T1 and U1) 0.1 V/A 0.5 V...4.5 V (−2 V...2 V)
3	T1: P8208NL U1: ACS723LLC-5AB-T R1: 2 × 100R parallel Gain adjustment U3A: Cutoff frequency adjustment:	(Pulse Electronics) (Allegro Microsystems) (various) gain 1.25 R4: 2.5 k; R5: 10 k C4: 470p; R13: 0R	current range sensitivity output voltage	−5 A...5 A (supply voltage limited) 0.5 V/A 0 V...5 V (−2.5 V...2.5 V)

The variable resistors RV3 and RV4 can be used to compensate systematic gain errors, but this requires calibration using a precision current source or a reference current sensor. Alternatively, if RV3 and RV4 are not populated, resistors R1, R4, R5, R6, R7, R8 and R15 should be selected as precision types with a tolerance $\leq 0.1\%$ to achieve high accuracy. The absolute value of R6, R7 and R8 also depends on the value of R1, as R7 is also loading the current transformer, and is effectively parallel to R1. This results in a reduced voltage VCT-VREF on the secondary side of the current transformer. Therefore, the resistance R7 should be much larger as R1. E.g. for R7 = 10 kΩ and R1 = 10 Ω than the loading effect of R7 will lead to an error of less than 0.1%.

3.6. Power and current consumption

As the sensor is either battery powered or integrated into a circuit, its power consumption is of major concern. Due to the linear voltage regulator used, the input power will be proportional to the input voltage and the current taken at the 5 V supply rail. A lower bound for this current can be estimated based on quiescent current values of ICs U1, U2 and U4, which are the major contributors regarding power consumption. Table 7 lists the typical and maximum values, taken from datasheets, and in Table 8 the current consumption is compared to three commercial PCB current sensors [23–25], showing that the proposed current sensor has a comparable input current.

4. Design files

The design files accompanying the current sensor are mainly the complete PCB design files (Table 9). For construction of the PCB and schematic drawing, KiCad [12] was used.

- *OS_Current_Sensor_Schematic.pdf* – Schematic of current sensor, exported to PDF from KiCad.
- *OS_Current_Sensor_Silkscreen.pdf* – Silkscreen exported from KiCad to PDF, to assist during assembly.
- *Current_Sensor_V4_SMD.zip* – Complete KiCad project as one zip-file, including all custom footprints and symbols.
- *Current_Sensor_V4_SMD.kicad_pcb* – KiCad PCB file of the project. Some PCB manufactures (e.g. [13,16]) just need this file to generate the manufacturing data. Otherwise you need to export Gerber files. A tutorial to generate Gerber Files from KiCad can be found at [9].
- *Current_Sensor_V4_BOM.ods* is the complete bill of materials in open office spreadsheet format. For all parts links to online catalogues of distributors are given.

Table 7
Quiescent current of major circuit components.

Component	Typ.	Max.
U1 ACS724LLC-20AB-T	10 mA	14 mA
U2 UA78L05	3.8 mA	6 mA
U4 AD8061	6.8 mA	9.5 mA
total quiescent current	20.6 mA	29.5 mA

Table 8
Comparison of current consumption to commercial PCB current sensors.

Sensor	Typ.	Max.
ACS730 (Allegro)	17 mA	25 mA
HLSR-P series (LEM)	19 mA	25 mA
LA01P (TAMURA)		10 mA
Proposed Current Sensor	20.6 mA	29.5 mA

Table 9
Design files.

Design file name	File type	Open source license	Location of the file
OS_Current_Sensor_Schematic.pdf	Schematic PDF	CC-BY-SA 4.0	https://osf.io/mek8n/
OS_Current_Sensor_Silkscreen.pdf	Silkscreen PDF	CC-BY-SA 4.0	https://osf.io/x42nq/
Current_Sensor_V4_SMD.zip	KiCad Project ZIP File	CC-BY-SA 4.0	https://osf.io/vfsqg/
Current_Sensor_V4_SMD.kicad_pcb	KiCad PCB file	CC-BY-SA 4.0	https://osf.io/p7mn6/
Current_Sensor_V4_BOM.ods	ods spreadsheet	CC-BY-SA 4.0	https://osf.io/9dre7/

5. Bill of materials

Given prices are based on single or low quantities as given in Table 10. The PCB price is given for manufacturing of 10 pieces at [13], but strongly depends on the PCB manufacturer. It is recommended to use a prototyping service like [13–16] to manufacture the PCB. All parts documented in the schematic are listed. For optional parts no values are assigned, as these depend on the particular circuit modifications. All components, except the PCB, can be bought at major distributors

Table 10
Bill of materials.

Designator	Component	Number	Cost per unit	Total cost	Source of materials/order no.
C1	Capacitor, 330 nF, 50 V, X7R, 0603	1	0.22 €	0.22 €	Mouser 810-CGA3E3X5R1H334MB
C2, C9	Capacitor, 1 µF, 16 V, X7R, 0603	2	0.08 €	0.16 €	Mouser 710–885012106017
C3, C5, C6	Capacitor, 100 nF, 50 V, X7R, 0603	3	0.05 €	0.15 €	Mouser 710–885012206095
C4	Capacitor, 2.2 nF, 50 V, X7R, 0603	1	0.08 €	0.08 €	Mouser 80-C0603C222K5RAUTO
C7	Capacitor, 10 µF, 35 V, X5R 0805	1	0.31 €	0.31 €	Mouser 81-GRM21BR6YA106KE3L
C8	Capacitor, 1 pF, 50 V, C0G, 0603	1	0.08 €	0.08 €	Mouser CC0603CRNPO9BN1R0
C11	Capacitor, 6.8 pF, 50 V, C0G, 0603	1	0.17 €	0.17 €	Mouser 80-CBR06C689B5GAC
C12	Capacitor, 220 pF, 50 V, C0G, 0603	1	0.08 €	0.08 €	Mouser 77-VJ0603A221JXACBC
C10, C13	Optional 0603 capacitors	–	–	–	–
J1, J2, J3	2 Position 2.54 mm pin header	3	0.15 €	0.45 €	Mouser 538–22-28–9020
J6	SMA PCB connector Molex	1	3.40 €	3.40 €	Mouser 538–73251-3140
R1	Resistor, 10R, 0.1%, 0.125 W, 0805	1	0.54 €	0.54 €	Mouser 603-RT0805BRD0710RL
R2	Resistor, 68 k, 1%, 0.1 W, 0603	1	0.09 €	0.09 €	Mouser 652-CR0603FX-6802ELF
R4, R6, R7, R8, R9, R10	Resistor, 10 k, 0.1%, 0.062 W, 0603	6	0.08 €	0.48 €	Mouser 284-APC0603B10K0N
R11	Resistor, 100R, 1%, 0.1 W, 0603	1	0.08 €	0.08 €	Mouser 603-AC0603FR-07100RL
R16, R17	Resistor, 24R, 1%, 0.1 W, 0603	2	0.08 €	0.16 €	Mouser 652-CR0603FX-24R0ELF
R18	Resistor, 0R, 5%, 0.1 W, 0603	1	0.08 €	0.08 €	Mouser 603-AC0603JR-130RL
R3, R5, R12, R13, R14, R15, R19	Optional 0603 resistors	–	–	–	
RV1	Trimmer resistor SMD 50 k	1	1.16 €	1.16 €	Mouser 858-23BR50KLFTR
RV2	Trimmer resistor SMD 1 k	1	0.84 €	0.84 €	Mouser 858-23BR1KLFTR
RV3, RV4, RV5	Optional trimmer resistor	–			
T1	P8208NL	1	2.07 €	2.07 €	Mouser 673-P8208NL
U1	ACS724LLC–20AB-T (SOIC8)	1	4.93 €	4.93 €	DIGIKEY 620–1720-1-ND
U2	UA78L05AIPK (SOT89)	1	0.30 €	0.30 €	Mouser 595-UA78L05AIPK
U3	MCP602ISN (SOIC8)	1	0.57 €	0.57 €	Mouser 579-MCP602ISN
U4	AD8061ARZ (SOIC8)	1	1.99 €	1.99 €	Mouser 584-AD8061ARZ-R7
	Custom made price depends on manufacturer and number of units (price here for 10 units)	1	5 €	5 €	Diverse PCB prototyping services, e.g. www.aetzwerk.de [13]
	Battery contact snap	1	0.57 €	0.57 €	Mouser 534-81-8 TB
	Rechargeable battery 9 V	1	6–10 €	6–10 €	various suppliers

like Mouser [17] or DIGIKEY [18]. The complete bill of materials, including part numbers for ordering and hyperlinks to distributor webpages can be found at: https://osf.io/9dre7/.

Total cost of hardware is about 25–35 €, dependent upon the cost for the custom PCB and the need for a 9 V battery.

6. Build instructions

To build the sensor, basic electronics assembly skills are needed, especially SMD component soldering. As the board is relatively small (40 mm × 35 mm) and has low component count, it can be easily hand soldered in less than 1 h. Smallest part size is 0603 package for most passive components. All ICs are SO type packages and the components are only mounted on the top side of the PCB, so the board is suitable for hand soldering. For manufacturing by hand, the following sequence for component soldering is recommended:

1. Start soldering the four ICs U1, U2, U3, and U4, beware of pin 1 orientation.
2. Solder all passive 0603 components you need. Beware of components marked as DNP (do not populate) in the schematic; these are only needed for modifications.
3. Mount the current transformer T1 and the trimmer pots RV1, RV2 and if needed RV3–RV5. Here the correct polarity of the secondary winding should be checked.
4. Last mount the coaxial connector J6 and if needed the pin headers J1, J2, J3, or otherwise connect wires for the needed interfaces.

As an alternative, some prototyping services offer the assembling of the boards at additional costs. Fig. 14 shows the silkscreen for placement of the components, and the top and bottom view of an unpopulated PCB.

7. Operation instructions

7.1. Safety concerns

Although input and output of the sensor are galvanic isolated, the current sensor should just be used for low DC voltages (<60 V), because the current transformer has just a functional isolation and no safety isolation. The sensor should never be used to measure current in a mains application. In case of failure, a potential lethal voltage can be accessible at the GND terminal of the oscilloscope and the secondary side of the sensor.

7.2. Basic connection setup

Fig. 15 shows an example setup used for calibration to show the connections needed for the sensor.

The operation of the sensor is straightforward, an isolated power supply (preferable a 9 V battery) should be connected to J3 to power the sensor. The positive power input is the upper pin of connector J3 (marked red in Fig. 15). To connect the output signal to an oscilloscope, a SMA to BNC adapter cable is used between J6 and the scope, having its input set to high impedance mode (e.g. 1 MΩ). The sensor has to be inserted, e.g. clamped or soldered or otherwise connected, between J1 and J2 in the circuit branch where the current is to be measured.

7.3. Calibration of sensor

An adjustment of the trimmer potentiometers RV1–RV4 (RV3 and RV4 are optional) is needed to properly use the sensor. The following characteristics are affected:

- RV1 sets the cutoff frequency of the Hall effect current sensor
- RV2 is used to compensate for a DC offset in the output signal
- RV3 and RV4 adjust the gain of the two sensor signal paths

To tune these trimmers, an experimental setup as depicted in Fig. 16a) or b) can be used. A signal/waveform generator and a reference probe, either a voltage probe as in Fig. 16a), or a wide bandwidth current probe, can be used. In both cases, the sensor output voltage $V_{S,out}$ is compared to the reference probe voltage V_{probe}.

Calibration can be performed in four steps, where step 2) and 3) are optional, as these can be only performed if RV3 and RV4 are populated.

1. Connect the power supply of the current sensor, and measure the output voltage without current flowing through the sensor terminals, i.e. signal generator is turned off. Now adjust trimmer RV2 until the voltage $V_{S,out}$ reaches 0 V or 2.5 V, in case the internal GND signal is connected to the output.
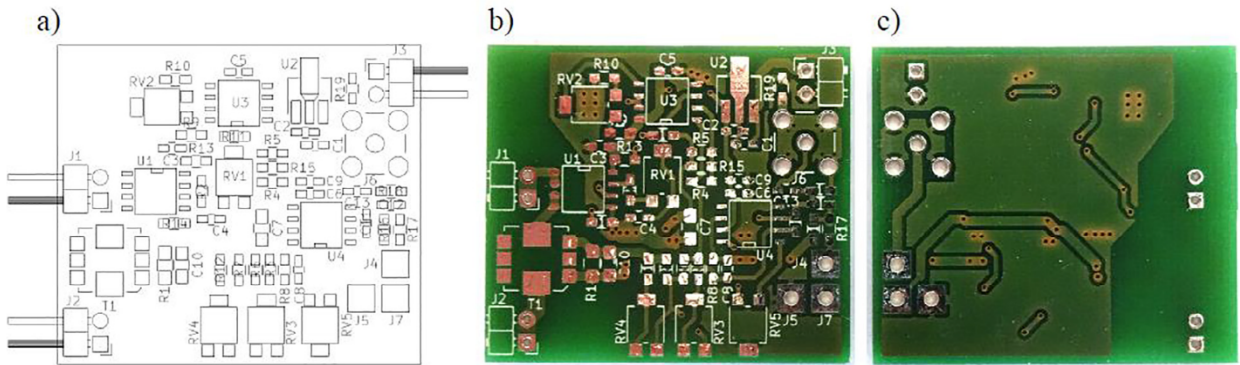
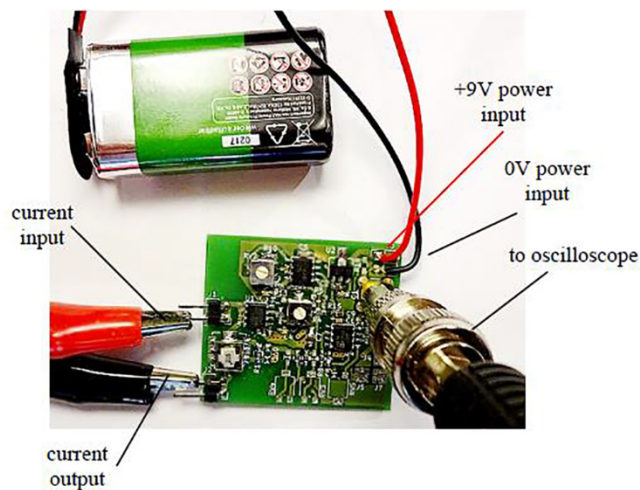**Fig. 14.** a) PCB silkscreen b) top and c) bottom view of unpopulated PCB.

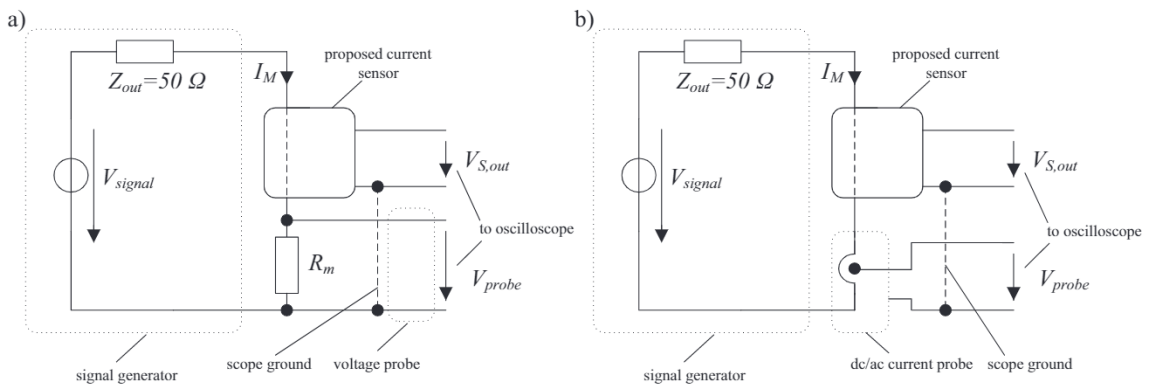**Fig. 15.** Connection setup of current sensor.

Fig. 16. Setup for calibration with a) voltage probe or b) current probe as reference.

2. (Optional) Turn the signal generator on, and set up a DC voltage. Measure the corresponding current and adjust RV3 until the measured value corresponds to the comparison value with the reference probe.

3. (Optional) Measure a high frequency sine wave (much larger than the cutoff frequency of the Hall sensor, e.g. 300 kHz), and adjust RV4 until measured value corresponds to the comparison value with another probe.

4. This last step adjusts the frequency compensation. There are two variants, 4a) is a fast method but not as accurate as 4b). For this reason procedure 4b) is recommended.
5. 4a) Set the signal generator for a low frequency (about 100 Hz) square wave signal; now try to adjust RV1 in a way normally used for compensating a voltage probe with a scope reference signal. This calibration step can be difficult, due to the low frequency noise of the Hall sensor, and the low signal levels delivered by typical lab waveform generators; therefore step 4b) is recommended.

4b) As an alternative, or to test if RV1 is set up properly, measure the amplitude of a sine wave for frequencies below and above the cutoff frequency of the Hall sensor, and test if the frequency response is flat, e.g. measure at 100 Hz, 500 Hz, 1 kHz, 2 kHz, 5 kHz and then at 10 kHz with a sine wave of constant amplitude. If there is a dip in the frequency response, the value of RV1 is too high; correspondingly if there is a peak in the frequency response, RV1 is too low in value.

7.4. Typical error

A common error is a too low supply voltage, especially when using a battery which has been discharged. If the measured values suddenly seem not to be accurate, or if offset and/or output voltage is drifting, then at first the power supply should be checked.

8. Validation and characterization

8.1. Current and power consumption

The current consumption is measured by replacing the battery with a variable lab power supply, which is varied from 7 V to 20 V. In Fig. 17 the measurement results are shown. The sensor draws a nearly constant input current of 22 mA–23 mA, slightly decreasing with decreasing supply voltage. Therefore power consumption increases nearly constant with increasing supply voltage. Sensor loading and input signal variations do not significantly change the current consumption.

8.2. DC transfer characteristics measurement

Fig. 18 depicts a simple setup for testing the DC accuracy of the proposed sensor.

A laboratory power supply with adjustable current limit is used as a variable current source. This supply generates a measurement current I_M flowing through the sensor and an in series connected digital multimeter (type used here: Fluke 27II). The multimeter is used to accurately measure the DC current, which is adjusted in 0.5 A steps from -10 A to $+10$ A. The output voltage of the sensor is measured using an oscilloscope, which is set to an averaging acquisition mode (64 averages) to filter out high frequency noise. Measurement results for a particular sensor are shown in Fig. 19. Left in Fig. 19a), the measured DC transfer characteristic is shown, which should be a linear curve with a slope of 0.1 V/A, representing the ideal sensor gain. Right in Fig. 19b), the relative error between the ideal and the measured values is shown, in this figure the value for $I_M = 0$ A has been omitted, because a non-zero offset voltage will lead to an infinite relative error.

In Table 11 statistical characteristics for the relative error, as depicted in Fig. 19b), are given.

As can be seen from the measurements, the sensor has a nearly linear but slightly lower slope as expected. This can be concluded from Fig. 19, as the relative error is approximately constant at -2.0% to -2.5% for measured currents with an absolute value greater than 1.5 A. For this particular unit, the output voltage of the linear voltage regulator was at
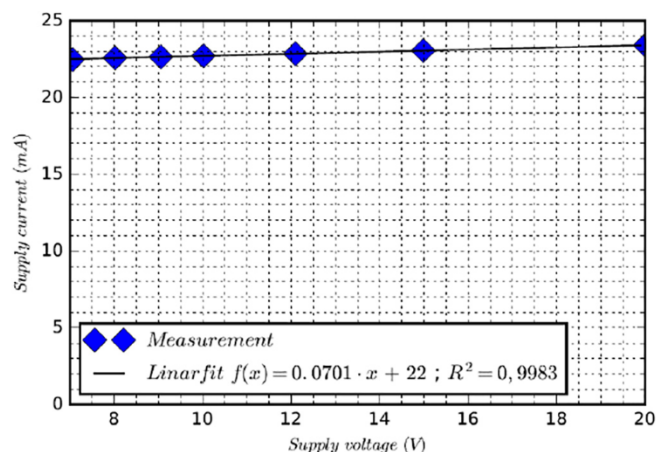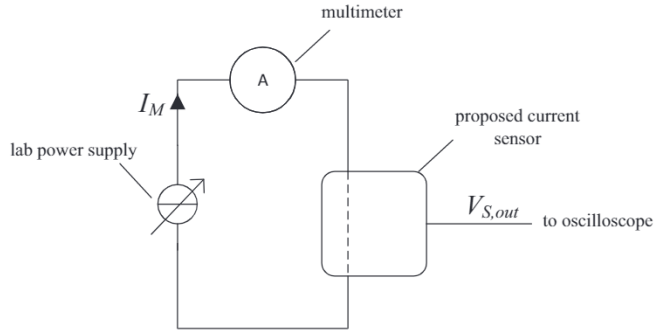

Fig. 17. Measured current consumption.

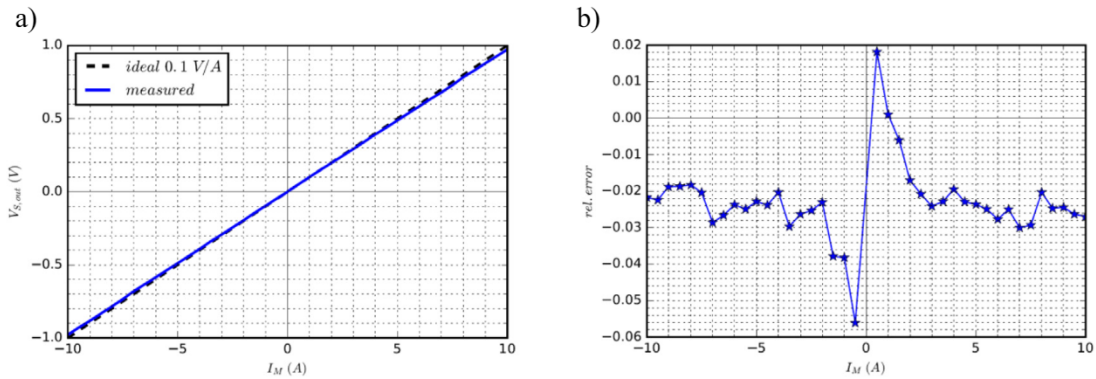Fig. 18. Experimental setup for measuring the DC characteristics.

Fig. 19. a) Measured DC transfer characteristic (blue) in comparison to ideal values (black) and b) relative error of measured transfer characteristic.

Table 11
Statistical characteristics for relative error of DC transfer characteristic.

Current range	Mean	Max value	Min value	Standard deviation	Standard error of mean
−2 A...2 A	−0.0199	0.0182	−0.0561	0.0225	0.0080
−5 A...5 A	−0.0220	0.0182	−0.0561	0.0145	0.0032
−10 A...10 A	−0.0231	0.0182	−0.0561	0.0106	0.0017

4.924 V and therefore approximately 1.5% less than expected. As the Hall sensor has a ratiometric output voltage, this explains most of the error. The used sensor in this experiment also did not have the two calibration trimmers RV3 and RV4; therefore the error could not be adjusted.

8.3. Insertion impedance measurement

In contrast to commercial current probes, the current sensor proposed here is not a clamp-on type and therefore acts as a frequency-dependent impedance $Z_{CT}(f)$, inserted into the circuit under test. $Z_{CT}(f)$ can be approximated as a series connection of a small resistance R_{CT} and an inductance L_{CT}:

$$Z_{CT}(f) = R_{CT} + j \cdot 2\pi \cdot f \cdot L_{CT} \tag{5}$$

In Fig. 20, the absolute value of the measured insertion impedance of the proposed sensor using an Omicron Bode 100 network analyzer is shown. Additionally, the measured values $Z_{CT,meas}(f)$ are compared to the calculated values $Z_{CT,calc}(f)$ when evaluating (5) for $R_{CT} = 6 \text{ m}\Omega$ and $L_{CT} = 18 \text{ nH}$. As shown in Fig. 20, the measurements justify the approximation (5).

8.4. Characterization using a signal generator

In the following section, a dynamic characterization for a variant of the proposed sensor using a signal generator is provided. The performance is compared to two commercial oscilloscope current probes [26,27]. Their characteristics are summarized in following Table 12.
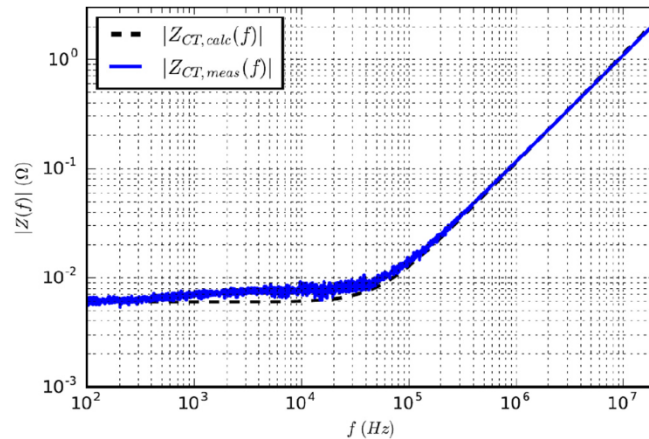
Fig. 20. Measured insertion impedance (blue) in comparison to calculated values (black).

Table 12
Current probes specifications.

Type	Current Range	Bandwidth	Sensitivity
LEM PR50 (same as Fluke i50s)	0…±3 A or 0…±30 (50 A for 10 s)	DC…50 MHz	1 V/A or 100 mV/A
Pearson Model 6298 (same as Model 2877)	0…±2.5 A (RMS) 0…±100 A (Peak)	300 Hz…200 MHz	1 V/A
Proposed Sensor	0…±10 A	DC…5 MHz	100 mV/A

8.4.1. Frequency response measurement

Fig. 21 shows the measured frequency response using a setup similar to calibrate the sensor, as previously shown in Fig. 16b). For comparison, the frequency response of the two commercial current probes (LEM PR50, Pearson Modell 6298/2877), which were measured simultaneously, are also depicted. The measurements were taken up to a frequency of 20 MHz; amplitude values are determined using the automatic measurement functions of the used oscilloscope. The bandwidth limit was set to 20 MHz and signal acquisition was set to averaging of eight subsequent waveforms to reduce noise. The nominal current level is about 100 mA amplitude (200 mA peak to peak) and was set by the output voltage of a signal generator.

In Fig. 22 the relative error of the frequency response is shown. The values here are taken from the average of three measurements from different oscilloscope channels. Signal amplitude was set to about 200 mA (400 mA peak to peak).

In Table 13 statistical characteristics for the relative error of the frequency response, as depicted in Fig. 22, are given.
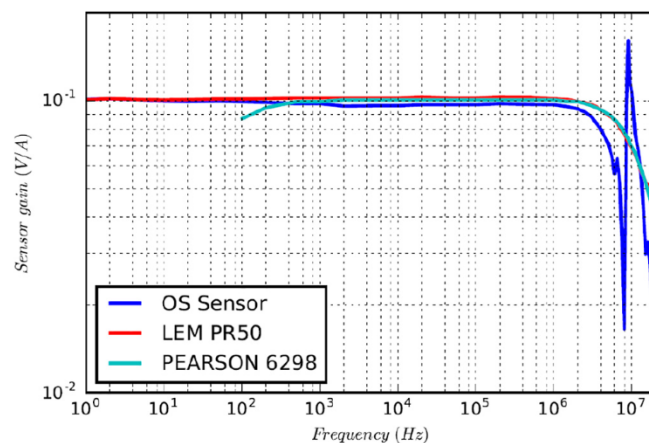

Fig. 21. Measured frequency response of proposed sensor (blue) vs. commercial sensors LEM PR50 (red) and Pearson model 6298 (cyan, values divided by factor 10).
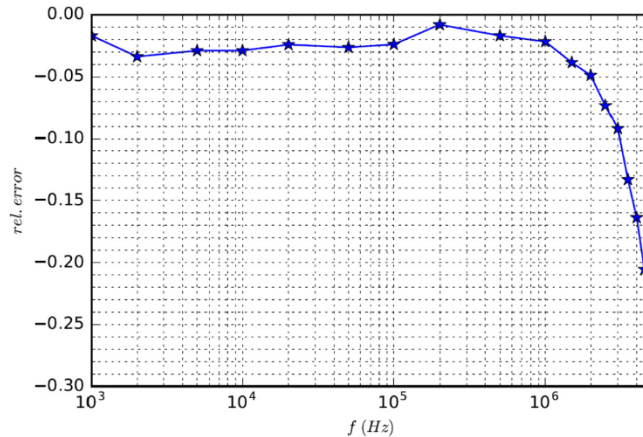
Fig. 22. Relative error of measured frequency response referenced to Pearson current monitor in the range 1 kHz–5 MHz.

Table 13
Statistical characteristics for relative error of frequency response.

Frequency range	Mean	Max value	Min value	Standard deviation	Standard error of mean
1 kHz…5 MHz	−0.0679	−0.0080	−0.2377	0.0682	0.0161
1 kHz…3 MHz	−0.0344	−0.0080	−0.0918	0.0221	0.0059
1 kHz…1 MHz	−0.0230	−0.0080	−0.0338	0.0071	0.0022

The following can be concluded from the measured values:

- The current sensor shows a flat frequency response up to 2 MHz.
- The −3 dB corner frequency of the proposed sensor is greater than 5 MHz for the sample used here.
- At high frequency, the sensor shows a resonant behavior due to parasitic capacitances and stray inductance, therefore the useable upper frequency is limited.
- Practical gain in the frequency region where the current transformer operates (above 1 kHz) is about 2%–3% lower as in the low frequency region covered by the Hall sensor. This systematic error can be adjusted if the trimmer pots RV3 and RV4 are populated.
- Besides the systematic gain error, an error less than 1% can be achieved for frequencies smaller than 1 MHz and less than 2.5% error can be achieved for frequencies smaller than 3 MHz.

One can observe an overall reduction in gain, also for the reference sensors. The reason for this is partly the set bandwidth limitation of 20 MHz, and partly a reduction in current amplitude of I_M, due to the fact, that not the current amplitude was set to a fixed value by the signal generator, but the voltage amplitude. Therefore, at higher frequencies the wires needed to connect the current sensors show frequency dependent impedance, which lowers the current at higher signal frequencies.

8.4.2. Pulse signal measurements

Figs. 23 and 24 show the comparison of the proposed sensor to two commercial current probes, while measuring square wave signals with varying frequency. The experimental setup remains the same, as previously shown in Fig. 16b). The output voltage level of the signal generator is set to a peak to peak value of 10 V, resulting in a current change of 200 mA (peak to peak). In Fig. 23 the rise and fall time was set to the minimum value of 4 ns each, but the displayed rise and fall times are limited by setting the oscilloscope to 20 MHz bandwidth. In Fig. 24 the rise and fall times are varied as indicated.

The sensor gain of the Pearson current monitor is 1 V/A compared to 0.1 V/A of the two other sensors, this is why the Pearson current sensor seems to have less noise compared to the other sensors. The results show that there is some low frequency noise in the output signal of the proposed current sensor, which can be attributed to the used Hall effect sensor. Further it can be observed that there is some ringing/overshoot for high signal frequencies, and fast rise times due to the resonant behavior of the current transformer.

8.5. Example application as current sensor in a lab experiment

To test the current sensor in a more realistic application, a DC/DC buck converter used for undergraduate lab experiments, was chosen as example. A simplified schematic is shown in Fig. 25. The current sensor was inserted in series to the output inductor. For comparison, a reference dc/ac current probe (LEM PR50) was also used to measure the same current.
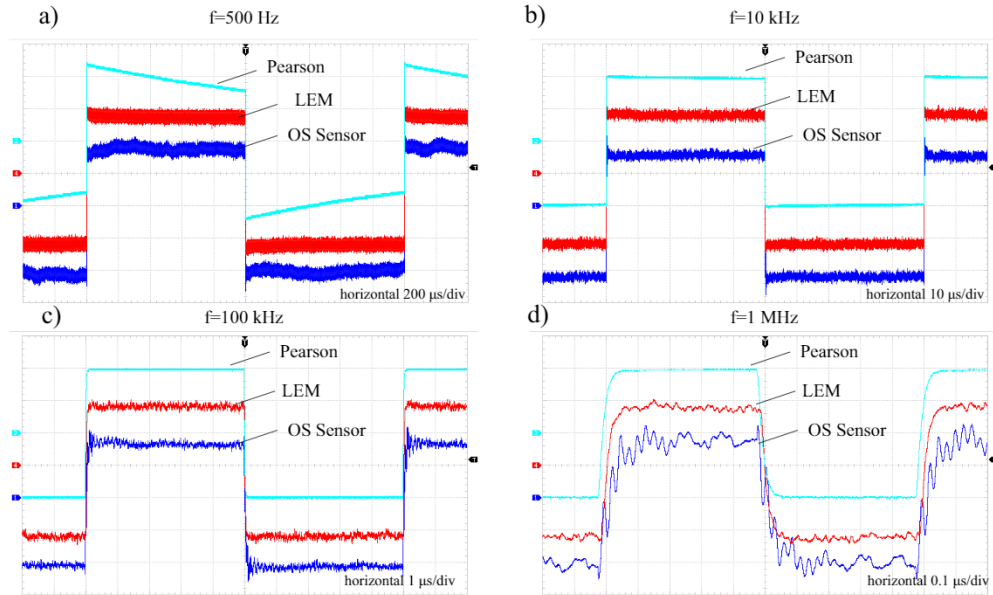
Fig. 23. Measured pulse response of square wave signals of proposed sensor (blue trace – OS sensor – 50 mA/div) compared to current probe LEM PR50 (red trace – LEM – 50 mA/V) and Pearson current monitor model 6298 (cyan trace – Pearson – 50 mA/div).
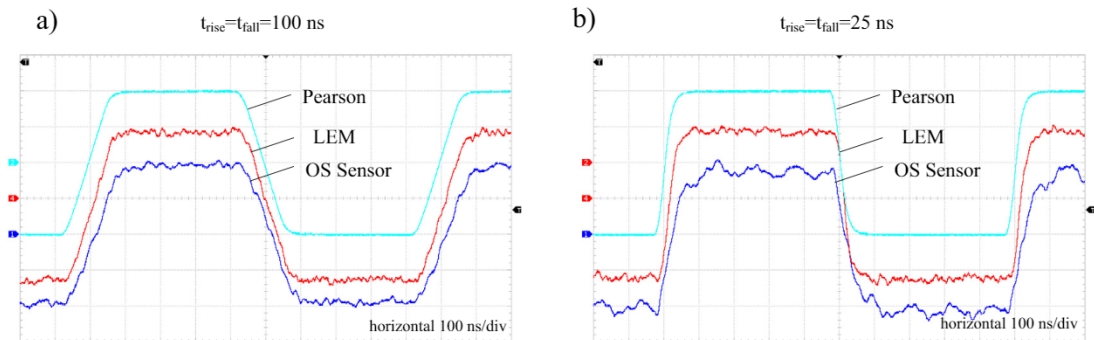
Fig. 24. Measured pulse response of square wave signal with f = 1 MHz and varied rise and fall times of proposed sensor (blue trace – OS sensor – 50 mA/div) compared to current probe LEM PR50 (red trace – LEM – 50 mA/V) and Pearson current monitor model 6298 (cyan trace – Pearson – 50 mA/div).

Some example results are shown in Figs. 26 and 27. In all cases input voltage is set to V_{IN} = 24 V, output voltage is V_{OUT} = 5 V, and the circuit is operating at a switching frequency of 100 kHz. Output current I_{OUT} is varied to produce different load conditions. In Fig. 26 waveforms for a) operation in continuous conduction mode (CCM) with a DC output current of 1 A and b) for a reduced load current of 0.1 A to force the converter to operate in discontinuous conduction mode (DCM) are shown.

In Fig. 27, a load step response is monitored with both current sensors. Summarizing the results of these measurements, it can be concluded that the proposed sensor is capable of delivering results comparable to a commercial current probe, and can be used as a viable replacement for an application where no absolute accuracy is needed, e.g. in educational lab experiments.

8.6. Testing summary and comparison

Sensor characterization regarding DC transfer characteristics, current consumption, insertion impedance and AC transfer characteristics have been described in the preceding sections. The resultant sensor characteristics are summarized in
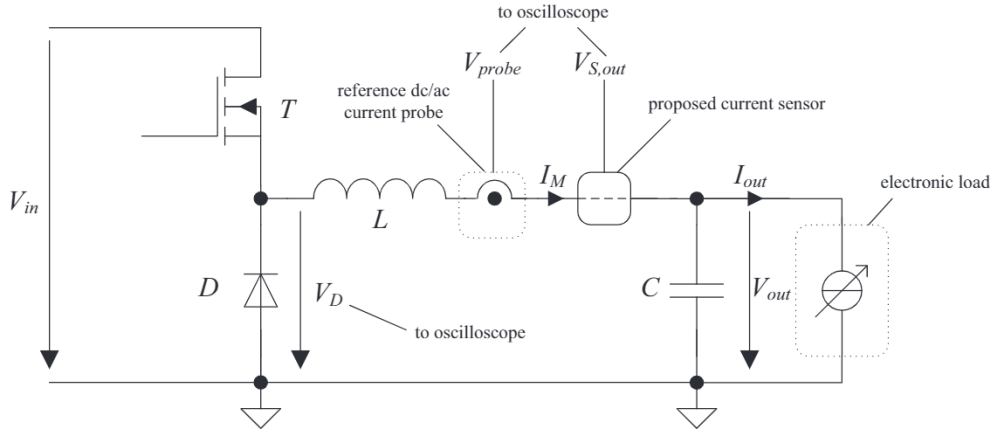
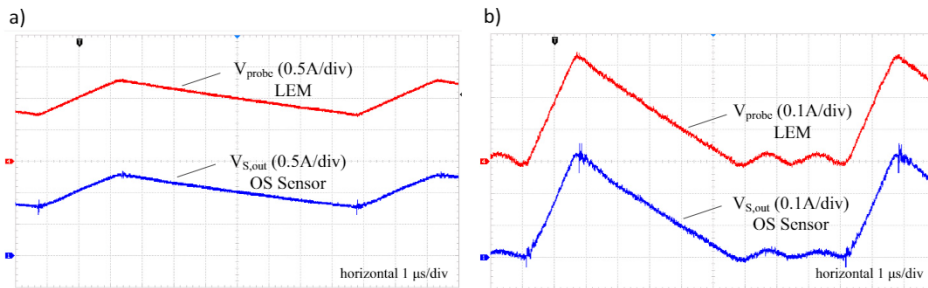**Fig. 25.** Test application circuit a 24 V to 5 V buck converter.

Fig. 26. Current waveforms for buck converter a) in CCM with I_{OUT} = 1 A and b) in DCM with I_{OUT} = 0.1 A for a test application circuit a 24 V to 5 V buck converter.
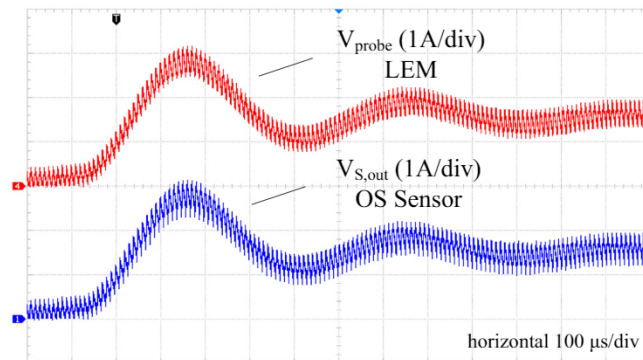

Fig. 27. Current waveforms for buck converter load step from I_{OUT} = 0.1 A to I_{OUT} = 1.5 A.

Table 14. For comparison the characteristics of several commercial current sensors, both ICs for circuit integration and oscilloscope probes, are also listed.

9. Improvements, limitations and modifications

Although the described sensor shows good measurement results, when compared to commercial sensors, there are some potential problems and/or limitations using this sensor. Therefore, some improvements are suggested:

Table 14
Testing summary and comparison to other probes.

Sensor	Characteristics Summary		
Proposed Sensor	Current Range	0…±10 A	(peak and RMS)
	Bandwidth (−3 dB)	DC…5 MHz	
	Sensitivity	0.1 V/A	
	Insertion Impedance	$Z(f) \approx 6\ m\Omega + j2\pi f \cdot (18\ nH)$	
		$|Z| < 0.02\ \Omega$	f < 0.1 MHz
		$|Z| < 0.2\ \Omega$	f < 1 MHz
	DC Accuracy*	−2.3%** ± 1.5%	of full scale value
	AC Accuracy*	−2.3%** ± 1%	1 kHz < f < 1 MHz
		−3.4%** ± 2.5%	1 kHz < f < 3 MHz
		*includes oscilloscope error	
		**systematic gain error which could be compensated	
ACS730KLCTR-20AB (Allegro)	Current Range	0…±20 A	
	Bandwidth (−3dB)	DC…1 MHz	
	Sensitivity	0.1 V/A	
	Insertion Impedance	not specified	
		primary conductor resistance < 1.2 mΩ, but additional PCB traces required	
	Accuracy	±4%	total Error
	Remarks:	current sensor IC; additional PCB required	
i-prober 520 (AIM TTI)	Current Range	±10 mA…±10 A	
	Bandwidth (−3dB)	DC…5 MHz	
	Sensitivity	1 V/A	(wire mode)
	Insertion Impedance	not specified	
	Accuracy	±5%	(full bandwidth)
	Remarks:	clamp on type current sensor, positional current and magnetic field sensor for oscilloscope	
N2893A (Keysight)	Current Range	0…±15 A (pulse 50 A for a pulsewidth <10 μs)	
	Bandwidth (-3dB)	DC…100 MHz	
	Sensitivity	0.1 V/A	
	Insertion Impedance	$|Z| < 0.01\ \Omega$	f < 0.1 MHz
		$|Z| < 0.02\ \Omega$	f < 1 MHz
	Accuracy*	±1% of reading ±1 mV	
		*probe only; not total accuracy; specified for low frequency (DC to 66 Hz)	
	Remarks:	Oscilloscope type probe for Keysight Oscilloscopes	
model 6298 (2877) (Pearson Electronics)	Current Range	0…±2.5 A (peak current 100 A)	
	Sensitivity	1 V/A	
	Bandwidth (−3dB)	300 Hz…200 MHz	
	Insertion Impedance	not specified	
	Accuracy	+1%…0%	

- Possible high frequency interferences caused by fast changing electrical fields may occur in the measurements. These interferences can be reduced by changing the orientation of the sensor, or making a better connection to earth using a voltage probe ground clip directly at the SMA jack J6, which is connected to an unused scope channel. The measurements documented in Figs. 24 and 25 were made using such a connection. A further improvement could be achieved by using a shielded case, connected to the output signal reference ground.
- There is some low frequency noise in the sensor output, generated by stray magnetic fields which are measured by the Hall effect current sensor. These are not inherent to the special design used here, but a generic problem with unshielded Hall effect current sensors. Some sort of magnetic shielding could improve the sensor output at low frequency.
- The upper bandwidth of the sensor is limited by parasitic effects of the used current transformer. The main limiting factor is assumed to be the coupling capacitance between primary and secondary winding. It should be possible to modify the sensor by using another type of current transformer for T1, or to use some custom wound current transformer to increase the bandwidth above 10 MHz.
- Another modification to try is to use a more precision linear voltage regulator to eliminate the need for a DC offset calibration.
- To improve the signal quality at higher frequencies, U4 could be replaced by an op amp which is capable to directly drive a 50 Ω terminated transmission at the output SMA connector; this could further eliminate reflections due to impedance mismatch.
- For use as standalone oscilloscope probe, a version with mounting holes, larger size and larger components (e.g. 0805 SMD components) could be designed. Also a circuit indicating low battery could be designed for this use case. Additionally, a 3D printed enclosure for this application could be designed.

Declaration of interest

None.

Funding acknowledgment

References

[1] A. Pinar, B. Wijnen, G.C. Anzalone, T.C. Havens, P.G. Sanders, J.M. Pearce, Low-cost open-source voltage and current monitor for gas metal arc weld 3D printing, J. Sens. 2015 (2015), https://doi.org/10.1155/2015/876714.

[2] G. Laimer, J.W. Kolar, Design and experimental analysis of a DC to 1 MHz closed loop magnetoresistive current sensor, in: Twentieth Annual IEEE Applied Power Electronics Conference and Exposition, 2005. APEC 2005, Austin, TX, 2005, pp. 1288–1292, https://doi.org/10.1109/APEC.2005.1453172.

[3] Low_Current_Sensor_Breakout-ACS712, 2018. https://github.com/. Available at: https://github.com/sparkfun/Low_Current_Sensor_Breakout-ACS712/tree/ACS723_v10 (accessed 05.07.2018).

[4] INA_169_Breakout, 2018. https://github.com/. Available at: https://github.com/sparkfun/INA169_Breakout (accessed 05.07.2018).

[5] L. Dalessandro, N. Karrer, J.W. Kolar, High-performance planar isolated current sensor for power electronics applications, IEEE Trans. Power Electron. 22 (5) (2007) 1682–1692, https://doi.org/10.1109/TPEL.2007.904198.

[6] N. Karrer, P. Hofer-Noser, A new current measuring principle for power electronic applications, in: Power Semiconductor Devices and ICs, 1999. ISPSD '99. Proceedings. The 11th International Symposium on, Toronto, Ont., 1999, pp. 279–282, https://doi.org/10.1109/ISPSD.1999.764117.

[7] Fried, L., 2018. https://www.adafruit.com/. Available at: https://learn.adafruit.com/adafruit-ina219-current-sensor-breakout/downloads (accessed 05.07.2018).

[8] Velsink, W.B., 1970. Inventor; Tektronix Inc. assignee. Magnetic field measuring method and device effective over a wide frequency range. US patent 3,525,041.

[9] PCBWay, 2018. https://www.pcbway.com. Available at: https://www.pcbway.com/blog/help_center/Generate_Gerber_file_from_Kicad.html (accessed 12.07.2018).

[10] N. Troester, J. Ruthardt, M. Nitzsche, J. Roth-Stielow, Wide bandwidth current sensor combining a coreless current transformer and TMR sensors, in: PCIM Europe 2018; International Exhibition and Conference for Power Electronics, Intelligent Motion, Renewable Energy and Energy Management, Nuremberg, Germany, 2018, pp. 1–7.

[11] ACS72X-Breakout, 2018. https://github.com/. Available at: https://github.com/watterott/ACS72X-Breakout (accessed 14.07.2018).

[12] KiCad EDA. http://kicad-pcb.org/ (accessed 14.07.2018).

[13] Aetzwerk GmbH. https://www.aetzwerk.de/ (accessed 14.07.2018).

[14] PCBWay. https://www.pcbway.com/ (accessed 14.07.2018).

[15] OSH Park. https://oshpark.com/ (accessed 14.07.2018).

[16] Multi CB. https://www.multi-circuit-boards.eu/ (accessed 14.07.2018).

[17] Mouser. https://www.mouser.com/ (accessed 14.07.2018).

[18] DIGIKEY. https://www.digikey.com/ (accessed 14.07.2018).

[19] RS Components. https://de.rs-online.com/ (accessed 24.11.2018).

[20] Fluke, 2018. 80i-110s AC/DC Current Probe Technical Data. Available at: https://www.tektronix.com (accessed 24.11.2018).

[21] Keysight, 2018. Keysight N2893A 100 MHz Current Probe User's Guide. Available at: https://www.keysight.com (accessed 24.11.2018).

[22] AIM-TTI, 2018. AIM-I-Prober 520 meter Datasheet. Available at: https://www.aimtti.com/ (accessed 24.11.2018).

[23] Allegro MicroSystems, 2018. ACS730 Datasheet. Available at: https://www.allegromicro.com/ (accessed 24.11.2018).

[24] LEM, 2018. HLSR-P series Datasheet. Available at: https://www.lem.com/ (accessed 24.11.2018).

[25] Tamura Corporation. LA01P series Datasheet. Available at: https://www.tamura-ss.co.jp/ (accessed 24.11.2018).

[26] LEM. 2019. PR50 Data Sheet. Available at: https://docs-emea.rs-online.com/webdocs/0238/0900766b80238ae6.pdf (accessed 03.01.2019).

[27] Pearson Electronics, 2019. Datasheet Current Monitor Modell 2877. Available at: http://pearsonelectronics.com/pdf/2877.pdf (accessed 0301.2019).

[28] P. Poulichet, F. Costa, E. Laboure, A new high-current large-bandwidth DC active current probe for power electronics measurements, IEEE Trans. Indus. Electron. 52 (1) (2005) 243–254, https://doi.org/10.1109/TIE.2004.841066.

[29] S. Ziegler, R.C. Woodward, H.H. Iu, L.J. Borle, Current sensing techniques: a review, IEEE Sens. J. 9 (4) (2009) 354–376, https://doi.org/10.1109/JSEN.2009.2013914.

[30] Allegro MicroSystems, 2019. ACS724 Datasheet. Available at: https://www.allegromicro.com/ (accessed 04.01.2019).